Thermodynamics of strongly interacting fermions in two-dimensional optical lattices

Ehsan Khatami and Marcos Rigol

Thermodynamics of Strongly Interacting Fermions in 2D Optical Lattices

Ehsan Khatami and Marcos Rigol

Department of Physics, Georgetown University, Washington DC, 20057 and
Kavli Institute for Theoretical Physics, University of California, Santa Barbara, CA 93106

We study finite temperature properties of strongly correlated fermions in two-dimensional optical lattices by means of numerical linked cluster expansions, a computational technique that allows one to obtain exact results in the thermodynamic limit. We focus our analysis on the strongly interacting regime, where the on-site repulsion is of the order or greater than the bandwidth. We compute the equation of state, double occupancy, entropy, uniform susceptibility, and spin correlations for temperatures that are similar or below the ones achieved in current optical lattice experiments. We provide a quantitative analysis of adiabatic cooling of trapped fermions in two dimensions, both by means of flattening the trapping potential and by increasing the interaction strength.

I. INTRODUCTION

Recent optical lattice experiments have opened a new venue for exploring the effects of strong correlations in quantum lattice models. For example, the superfluid–Mott-insulator transition for bosons has been observed in three- [1], two- [2], and one- [3] dimensional geometries. Currently, there is a race to access temperatures low enough where the transition to the antiferromagnetically ordered Néel state in three dimensions (3D), or possibly more exotic states in two dimensions (2D), can be observed for fermions [4, 5]. So far, the interaction strength and the temperature in lattice fermion experiments remains relatively high in comparison to the hopping amplitude, t. This is in part because t, which is set by optical lattice parameters, is in general small in the regimes where one-band models are applicable.

On the theoretical side, there is an ever increasing demand for precise numerical results for the relevant parameters of the Hubbard model and for large enough system sizes, which could be used to interpret current experiments and also provide suggestions for future experiments [6–11]. For this model, especially for strong interactions, present computations become particularly challenging as the temperature is lowered below the hopping amplitude.

Here, we study various thermodynamic quantities such as the equation of state, entropy, double occupancy, and spin correlations in the thermodynamic limit for interactions up to three times the bandwidth, utilizing numerical linked cluster expansions [13, 14]. We provide a detailed understanding of the evolution of various quantities with adiabatically increasing the interaction strength, of great interest to current optical lattice experiments. Using the local density approximation (LDA), we analyze the thermodynamics of fermions in a harmonic trap and calculate their temperature as a function of the interaction strength and total entropy, as well as present a quantitative analysis of various cooling schemes for the experiments [15–17].

II. MODEL

We consider the 2D Hubbard Hamiltonian:

$$\hat{H} = -t\sum_{\langle i,j\rangle}(\hat{c}_i^\dagger \hat{c}_j + \text{H.c.}) + U\sum_i \hat{n}_{i\uparrow}\hat{n}_{i\downarrow} + \sum_i V_i \hat{n}_i, \quad (1)$$

where $\hat{c}_{i\sigma}^\dagger$ ($\hat{c}_{i\sigma}$) creates (annihilates) a fermion with spin σ on site i, and $\hat{n}_{i\sigma} = \hat{c}_{i\sigma}^\dagger\hat{c}_{i\sigma}$ is the number operator. $\langle ..\rangle$ denotes nearest neighbors (NN), U is the strength of the onsite repulsive interaction, and V_i is a space dependent local chemical potential. $t = 1$ ($\hbar = 1$ and $k_B = 1$) sets the energy scale throughout this paper.

III. COMPUTATIONAL APPROACH

In linked-cluster expansions [12], we express an extensive property of the model per lattice site in the thermodynamic limit (P) in terms of contributions from all the clusters, up to a certain size, that can be embedded in the infinite lattice:

$$P = \sum_c L(c)w_p(c), \quad (2)$$

where c represents the clusters. This contribution is proportional to the weight of each cluster for that property $[w_p(c)]$, and to its multiplicity $[L(c)]$. The latter is defined as the number of ways that particular cluster can be embedded in the infinite lattice, per site. The weight on the other hand, is calculated recursively as the property for each cluster $[\mathcal{P}(c)]$, minus the weights of all its subclusters,

$$w_p(c) = \mathcal{P}(c) - \sum_{s\subset c} w_p(s). \quad (3)$$

Here, we use the *numerical* linked-cluster expansion (NLCE), where $\mathcal{P}(c)$ is computed by means of full exact diagonalization [13]. Because of the exact treatment of individual clusters in NLCE, the series converges at significantly lower temperatures in comparison to high-temperature expansions in which perturbation theory is used.

NLCEs are complementary to quantum Monte Carlo (QMC) approaches, such as the determinantal QMC (DQMC) [18], or dynamical mean-field theory [19] and its cluster extensions such as the dynamical cluster approximation (DCA) [20, 21]. They can also help benchmarking future experiments as well as new computational techniques. This is because NLCEs do not suffer from statistical or systematic errors, such as finite size effects, and, as opposed to DQMC and DCA, they are not restricted to small or intermediate interaction strengths. In Ref. [22], we have made our raw NLCE data for a wide range of interactions available for comparison.

The validity of NLCEs, however, is limited to a region in temperature in which the series converge (the convergence region). The lowest temperatures at which NLCEs converge extend beyond those achievable with high temperature expansions [13]. We have found that, for the Hubbard model, NLCEs converge down to lower temperatures as the strength of the interaction is increased. At half filling, and for interactions larger than the bandwidth, NLCEs can access the region with strong AF correlations, identified by the suppression of the uniform susceptibility. Although, the method does not have any systematic restriction away from half filling, in the latter region, the series fail to converge at temperatures as low as those accessible to the half-filled case. This prevents us to access low-temperature phases, such as d-wave superconductivity, that arguably exist in this model at finite doping.

We begin our analysis with the homogeneous system ($V_i = 0$) in the grand canonical ensemble. For each U, we compute all properties for a very dense grid of chemical potential (μ) and temperature, so that we can also follow properties at constant density (n) [14]. The NLCE calculations are carried out on the square lattice up to the ninth order in the site expansion (nine sites). We use Wynn and Euler algorithms for summing the terms in the series to extend the region of convergence [13]. Since only NN hopping is considered, all properties of the particle-doped system can be expressed in terms of those from the hole-doped system. Hence, away from half-filling, we only show results for the hole-doped system.

IV. RESULTS

A. Equation of State

The equation of state for the Hubbard model provides important information about correlation effects as the strength of the on-site interaction is increased, and can be studied in optical lattice experiments. In Figs. 1(a)-(c), we depict the equation of state at three different temperatures, $T = 0.82$, 0.55, and 0.25 for the weak, intermediate, and strong coupling regimes ($U = 4$, 8 and 12, respectively). For the last two values of U [Figs. 1(b) and 1(c)], one can see the emergence of an incompressible region around $\mu = U/2$, a clear signature of the Mott gap
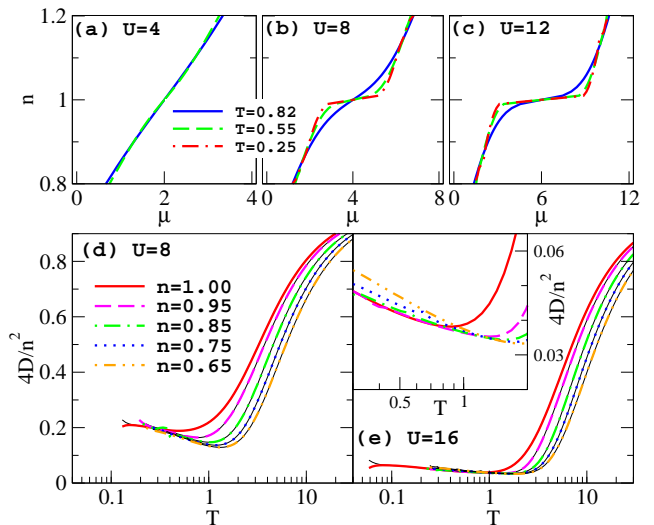

FIG. 1. (Color online) Top panels: Equation of state for (a) $U = 4$, (b) $U = 8$, and (c) $U = 12$ and at three different temperatures. Except for $U = 4$ at $T = 0.25$, NLCE results converge for all the values of chemical potential presented here. Only the last order of the series is shown after using Wynn sums with three cycles of improvement. Bottom panels: Normalized double occupancy vs T at four different hole doping for (d) $U = 8$ and (e) $U = 16$. We use Euler sums for the last 6 terms at half filling and Wynn sums for $n \neq 1$. Thin (black) lines in (d) and (e) are the results for the one to last order. The inset in (e) magnifies the low-temperature region for $U = 16$. The unit of energy is set to the hopping amplitude, t.

opening in the density of states at low temperatures.

B. Double Occupancy

In Figs. 1(d) and 1(e), we show the double occupancy, $D = \langle \hat{n}_\uparrow \hat{n}_\downarrow \rangle$, normalized by its uncorrelated high-temperature value ($n^2/4$) for $U = 8$ and 16, respectively. The double occupancy exhibits a clear low-T rise by decreasing temperature. This feature has attracted a lot of attention recently, especially after the real-space DMFT study of the 3D version of the model in a harmonic trap [9]. Gorelik *et al.* argued that the onset of the AF ordering in the strong-coupling regime is signaled by an enhanced double occupancy, which can be directly measured in optical lattice experiments. However, according to Fig. 1(d) and 1(e), the low-temperature rise occurs not only at half filling, but also away from it. Moreover, the rise starts at even higher temperatures for larger dopings. This implies that the enhancement of D in the trap by lowering the temperature is significant in the Mott insulating core as well as in other areas of the trap where density is less than one. Therefore, in real experiments, such an enhancement can be observed in systems that have a very small or even no Mott insulating region at the center of the trap. Hence, the increase in D alone
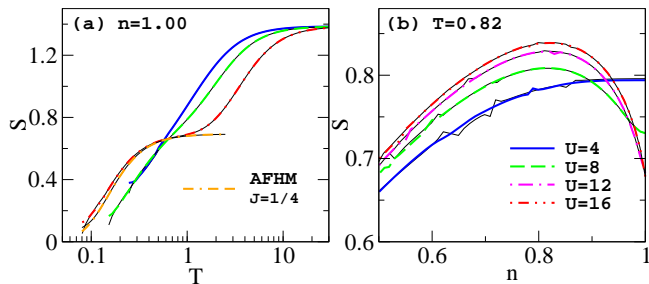
FIG. 2. (Color online) Entropy (a) vs T at half-filling, and (b) vs n at $T = 0.82$ for different U. Thick (thin) lines are results for the last (one to last) order of the sums as explained in Fig. 1. In (a), we have also included the entropy for the AFHM with the exchange interaction $J = 0.25$.
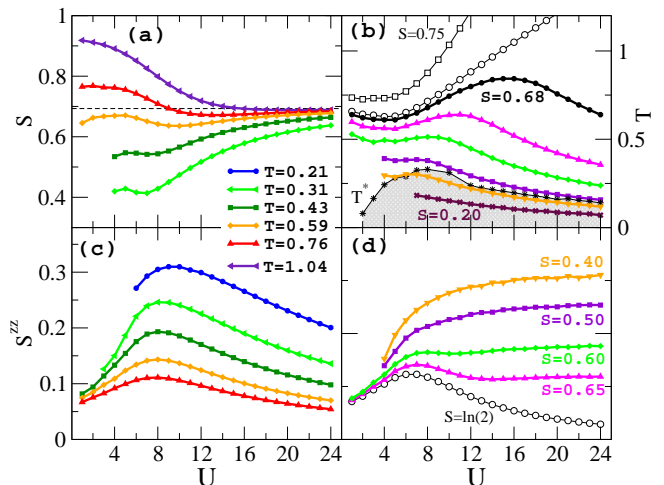

FIG. 3. (Color online) Interaction dependence of different quantities at half filling. Left panels: (a) Entropy and (c) NN spin correlations at fixed temperatures. Right panels: (b) Temperature and the (d) NN spin correlations at constant entropies. In (b), T^* represents a crossover temperature to the region where AF correlations grow exponentially by decreasing temperature (shaded area).

does not guarantee AF order. One has to also make sure that density is one in most of the trap.

For large values of U [see, e.g., $U = 16$ in Fig. 1(e)], the normalized D is almost independent of doping below $T \sim 1$ and down to the lowest accessible temperatures for $n \gtrsim 0.85$ (see inset), implying that $D \propto n^2$ in this region. One can understand the latter from the fact that local moments are likely ordered, and the double occupancy arises from virtual hoppings to NN sites, so, a relatively small number of extra holes only modifies the probability of those hoppings (accounted for by n^2), not the actual process.

C. Entropy

Generally, when using QMC-based methods, entropy calculations involve numerical derivatives and/or integration by parts [23, 24], which can introduce systematic errors. Within NLCEs, the entropy is computed directly from its definition in the grand canonical ensemble:

$$S = \ln(Z) + \frac{\langle \hat{H} \rangle - \mu \langle \hat{n} \rangle}{T}, \qquad (4)$$

where Z is the partition function.

We first study the entropy at half filling. Results are shown in Fig. 2(a) as a function of the temperature for $U = 4$, 8 and 16. There are two distinct regions of fast decrease in the entropy in the strong-coupling regime, e.g., $U = 16$. Those regions are separated by a crossing point of curves for different U around $T = 0.6$, corresponding roughly to $S = \ln(2)$. The emergence of these two regions results from the fact that as U increases, charge degrees of freedom are suppressed at higher temperatures due to the higher price of double occupancy, and, at the same time, the characteristic energy scale of the spin degrees of freedom, $J = 4t^2/U$, becomes smaller, pushing the low-T drop to lower temperatures. We find that in the latter region, the entropy curves for large U ($\gtrsim 14$) follow very closely the entropy of the antiferromagnetic Heisenberg model (AFHM). This is shown for $U = 16$ in

Fig. 2(a) where we also plot the entropy of the AFHM with $J = 0.25$.

In Fig. 2(b), we show the entropy away from half filling for a range of interactions at a fixed $T = 0.82$. In the weak-coupling regime (e.g., $U = 4$), the entropy increases monotonically with density and is maximal at half filling. Since correlations play a small role, the system behaves similarly to a non-interacting system, i.e., the closer to the point where there is an equal number of electrons and holes, the larger the entropy. This trend changes upon increasing U for which the moment ordering suppresses the entropy significantly close to half filling. As a result, there is a maximum in the entropy in the vicinity of the optimal doping for all interactions in the strong-coupling regime [25]. Below, we discuss how these features are reflected in the properties of trapped systems.
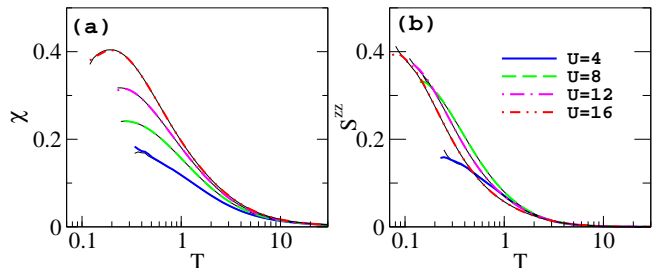
We further take advantage of the fact that, within NL-

FIG. 4. (Color online) (a) Uniform spin susceptibility and (b) NN spin correlations at half filling vs temperature for different interactions. χ peaks at T^* below which AF correlations grow exponentially with decreasing temperature. S^{zz} also shows a sharp increase around T^*.
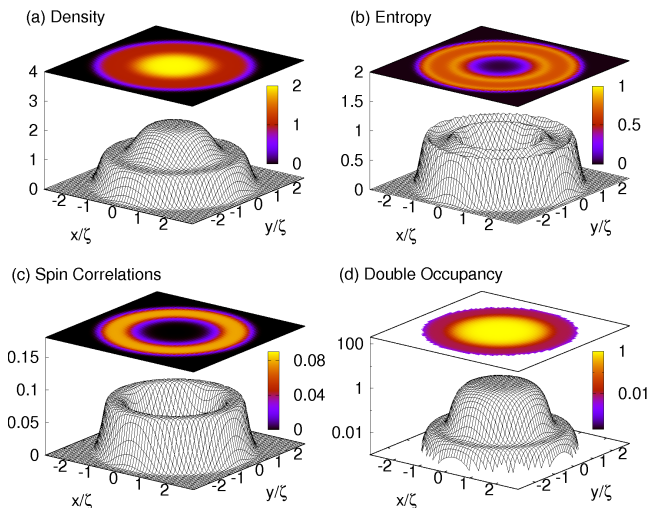
FIG. 5. (Color online) (a) Density, (b) entropy, (c) NN spin correlations, and (d) double occupancy profiles of fermions in a harmonic trap with $\tilde{\rho} = 22.9$, governed by the Hubbard model with $U = 16$ at $T = 0.76$. The average entropy per particle is $s = 0.56$.

CEs, arbitrary values of U can be studied at no additional computational cost, and determine the dependence of the quantities of interest on U. In Fig. 3(a), we show S at half filling as a function of U at fixed temperatures. The temperature regions identified for the entropy in Fig. 2(a) are more clearly seen in Fig. 3(a), i.e., the entropy stays more or less the same for $T \sim 0.6$ (the crossing point) as U increases whereas it generally decreases (increases) with U for $T > 0.6$ ($T < 0.6$).

The possibility of adiabatic cooling with increasing U in optical lattices has been studied by a number of groups recently [7, 23, 26]. Considering interactions that are often no larger than $3/2$ of the bandwidth, they argue that this process is rather weak in 2D. Here, we revisit the problem by including results for values of U up to three times the bandwidth [see Fig. 3(b)]. We find that starting from relatively large values of entropy below $\ln(2)$ (e.g., $S = 0.68$), accessible to current 2D experiments, and continuing to increase U, the half-filled system can be cooled down to very low temperatures. For smaller entropy, e.g., $S = 0.4$, one can even access the region with exponentially large AF correlations below the crossover temperature, T^*, as shown in Fig. 3(b). We take T^* as the temperature where the uniform spin susceptibility (χ) as a function of temperature peaks [7]. We find that T^* also coincides with the temperature at which the NN spin correlations, $S^{zz} = |\langle \sum_{\langle ij \rangle} S_i^z S_j^z \rangle|$, show a rapid growth by decreasing temperature. The uniform spin susceptibility and the NN spin correlations are depicted in Fig. 4. For $U \gg 1$, T^* is expected to scale with the AF exchange constant (J) in the effective Heisenberg model i.e., $\propto 1/U$. This behavior is observed in Fig. 3 (b), not only for T^*, but also for the large-U tails of the isentropic curves when $S < \ln(2)$, as J is the only energy
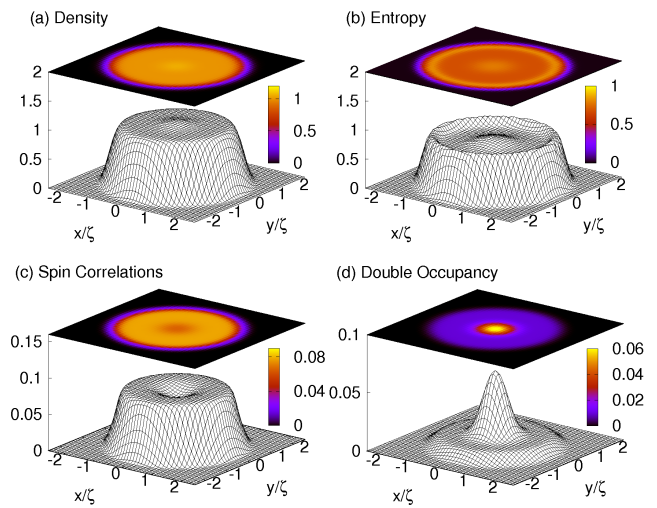

FIG. 6. (Color online) Same as Fig. 5 but for $\tilde{\rho} = 10.8$. The average entropy per particle is $s = 0.85$ in this case.

scale in that region. For $U < 12$ in the weak-coupling regime, T^* is not accessible to our NLCE. Therefore, we have taken T^* from the DQMC results of Ref. 7 for that region. It is interesting to see that this crossover temperature peaks when the value of the interaction is around the bandwidth.

D. Nearest-neighbor Spin Correlations

What is perhaps more important from the experimental point of view is how AF correlations change during the process of adiabatically increasing U. As mentioned in the introduction, one of the current main goals in cold fermion experiments is achieving AF in the Mott insulating state. However, the challenge in this case not only resides in realizing such a state but also in detecting it. Very recently, experimental breakthroughs have been reported which allow the detection of NN spin correlations [27, 28].

NN spin correlations, S^{zz}, can also be computed exactly using NLCEs. As expected, we find that S^{zz} is largest at half filling for all interactions. Therefore, we focus on the half-filled system and plot this quantity per site vs U at constant temperatures in Fig. 3(c), and at constant entropies in Fig. 3(d). The dependence of S^{zz} on U at constant T is non trivial. As the temperature is lowered to $T \sim 0.3$, a peak develops in the spin correlations around $U = 8$, which is indicative of the largest effective exchange interaction between NN spins. The peak is a result of the interplay between weak moment formation in the weak-coupling regime ($U < 8$) and the $1/U$ decrease of the effective J in the strong-coupling regime. We find that at lower temperatures ($T = 0.21$), the maximum of S^{zz} occurs at $U \sim 9$, which is not expected to change significantly by further decreasing temperature.

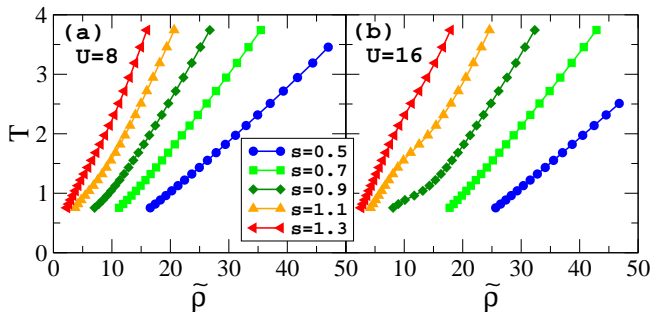At constant entropy, on the other hand, this picture is

FIG. 7. (Color online) Temperature vs characteristic density at constant entropies per particle for (a) $U = 8$ and (b) $U = 16$.

FIG. 8. (Color online) Temperature vs U at constant entropies per particle for (a) $\tilde{\rho} = 10.8$ and (b) $\tilde{\rho} = 22.9$. The shaded area, the same as in Fig. 3(b), is the region of exponentially large AF correlations below T^* in the Mott insulating core of the trap.

strongly modified. Figure 3(d) shows that S^{zz} saturates to a finite entropy-dependent value by increasing U along the isentropic paths of Fig. 3(b), provided that $S < \ln(2)$. Notice that, even though adiabatic cooling may not be efficient to arrive at regions with large AF correlations in 2D [23], the value of the NN spin correlations will be maximal in the large-$U(\gg 12)$ region if $S < 0.6$. This is convenient for experiments in optical lattices for which U is typically large compared to the bandwidth.

E. Trapped Systems

To make direct contact with experiments in optical lattices, we study the manifestation of our previous results in systems confined by a spatially varying harmonic potential, $V_i = V r_i^2$. Here, r_i denotes the radial distance of each site to the center of the trap, and for any given value of U, all properties of the system are determined by the characteristic density $\tilde{\rho} = N(V/2dt)^{d/2}$ [29], where d is the dimensionality and N is the number of particles. The resulting inhomogeneous Hubbard model is then studied using the local density approximation (LDA) along with our results for the infinite system. A recent QMC study of the inhomogeneous Hubbard model [11] has shown that the LDA is a good approximation for local observables at the temperatures accessible here. We should stress that NLCEs are ideal for this kind of studies because, for each value of U, one can compute all properties for a very dense grid of temperatures and chemical potentials at almost no additional computational cost. The same is of course not true for QMC-based calculations where each temperature and chemical potential requires a separate computation.

In Fig. 5(a), we plot the resulting density profile for $U = 16$ at $T = 0.76$. We have chosen $\tilde{\rho} = 22.9$ such that there are band- ($n = 2$) and Mott-insulating ($n = 1$) domains in the trap. Very useful information for the experiments is provided by the spacial distribution of the density, entropy, NN spin correlations, and double occupancy as shown in Figs. 5(b-d). The entropy is minimal (zero) in the band insulator, peaks at $n \sim 1.18$ and 0.82,
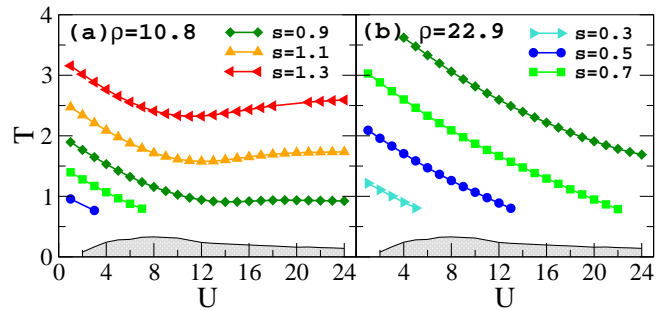
consistent with Fig. 2(b), and has a local minimum in the Mott ring. In the latter region, spin correlations are maximal, and as expected for this large value of U, the double occupancy is large only in the region where $n > 1$.

In Fig. 6, we show the same quantities as in Fig. 5, for a reduced $\tilde{\rho}$ of 10.8 at the same temperature and interaction strength. As a result of this isothermic change, the entropy per particle increases from 0.56 to 0.85. Nevertheless, the Mott-insulating region with relatively uniform entropy profile is clearly seen over most of the trap.

It has become apparent in experiments with fermions in optical lattices that cooling approaches beyond the standard evaporative cooling techniques are required if one is to reach low enough temperatures at which exotic physics emerges. Three recent proposals have shown how to generate low entropy states where a large fraction of the system is in a band insulating domain (i.e., with large values of $\tilde{\rho}$) [16, 17, 30]. The idea is then that one can adiabatically reduce the trap strength (the characteristic density $\tilde{\rho}$) so that the effective temperature of the fermions decreases. This way, antiferromagnetism and other low-temperature phenomena can be explored.

In Fig. 7, we show quantitatively how this idea works for trapped 2D systems. We plot the temperature as a function of $\tilde{\rho}$ for various values of the total entropy per particle. Recent studies have shown that the entropy per particle (s) for a particular U can be estimated by fitting the double-occupancy measurements at different $\tilde{\rho}$ to data from numerical simulations [8]. In Figs. 7(a) and 7(b) one can see that, for the two values of U shown, the temperature decreases rapidly with decreasing $\tilde{\rho}$, making evident that this approach works very efficiently for 2D trapped systems. The inflection point, seen e.g., for $s = 0.9$ in Fig. 7(b), is the signature of a large Mott region forming in the trap (as seen in Fig. 6). This occurs provided the entropy is low enough and for a range of characteristic densities that depends on U. AF ordering in the Mott core emerges at T^*, which for small entropies, can be reached before the Mott insulator is destroyed by further flattening of the trap.

It is also interesting to study what happens to the tem-

perature of a trapped system as one increases the interaction strength at constant entropy. [Results for homogeneous systems at half filling were presented in Fig. 3(b).] In Fig. 8, we show isentropic curves in the $T - U$ plane for trapped systems at various entropies and for the two characteristic densities, $\tilde{\rho} = 10.8$ and 22.9, used in Figs 5 and 6. As expected from the results in Fig. 7, the shape and location of the isentropic curves depend strongly on the value of $\tilde{\rho}$. In Fig. 8, we also show the same shaded area as in Fig. 3(b) below T^*, which here, represents the region where the Mott insulating core of the trap develops large AF correlations. Our calculations show that cooling can take place in trapped systems as the interaction increases. The entropies for which cooling is observed, and the values of U for which cooling occurs, depends on the characteristic density in the trap. Hence, as reported in Ref. [31] for three dimensional systems, adiabatically increasing the interaction strength can allow experimentalists to reach the temperatures needed to observe the onset of (quasi-)long-range antiferromagnetic correlations in a trapped system. Unfortunately, unlike for the homogeneous system at half filling, our NLCEs do not provide access to the temperatures relevant to that region for the 2D trapped system.

V.   SUMMARY

In summary, utilizing NLCEs, which within the convergence temperature region are free of statistical and/or systematic errors and provide exact results in the thermodynamic limit, we have calculated thermodynamic properties, such as the equation of state, double occupancy, entropy, uniform susceptibility, and NN spin correlations, of the 2D Hubbard model for a wide range of interaction strengths and temperatures. Precise data for the entropy on a dense temperature grid allowed us to study temperature and NN spin correlations, relevant to optical lattice experiments, as a function of the entropy. We find that for any $S < \ln(2)$, by adiabatically increasing U to very large values, the temperature decreases as $1/U$ and the spin correlations saturate to an entropy-dependent value beyond $U \sim 12$. Using the LDA, we have discussed the implications of our results for lattice fermions in the presence of a confining harmonic potential. In particular, we have shown how cooling can be achieved by reducing the confinement strength in a system that starts with a wide band insulating domain in the center of the trap, or by adiabatically increasing the interaction strength.

[1] M. Greiner, O. Mandel, T. Esslinger, T. Hansch, and I. Bloch, Nature **415**, 39 (2002), ISSN 0028-0836.

[2] I. B. Spielman, W. D. Phillips, and J. V. Porto, Phys. Rev. Lett. **98**, 080404 (2007).

[3] T. Stöferle, H. Moritz, C. Schori, M. Köhl, and T. Esslinger, Phys. Rev. Lett. **92**, 130403 (2004).

[4] R. Jordens, N. Strohmaier, K. Gunter, H. Moritz, and T. Esslinger, Nature **455**, 204 (2008).

[5] U. Schneider, L. Hackermller, S. Will, T. Best, I. Bloch, T. A. Costi, R. W. Helmes, D. Rasch, and A. Rosch, Science **322**, 1520 (2008).

[6] R. W. Helmes, T. A. Costi, and A. Rosch, Phys. Rev. Lett. **100**, 056403 (2008).

[7] T. Paiva, R. Scalettar, M. Randeria, and N. Trivedi, Phys. Rev. Lett. **104**, 066406 (2010).

[8] R. Jördens, L. Tarruell, D. Greif, T. Uehlinger, N. Strohmaier, H. Moritz, T. Esslinger, L. De Leo, C. Kollath, A. Georges, et al., Phys. Rev. Lett. **104**, 180401 (2010).

[9] E. V. Gorelik, I. Titvinidze, W. Hofstetter, M. Snoek, and N. Blümer, Phys. Rev. Lett. **105**, 065301 (2010).

[10] S. Fuchs, E. Gull, L. Pollet, E. Burovski, E. Kozik, T. Pruschke, and M. Troyer, Phys. Rev. Lett. **106**, 030401 (2011).

[11] S. Chiesa, C. N. Varney, M. Rigol, and R. T. Scalettar, Phys. Rev. Lett. **106**, 035301 (2011).

[12] H. C. Oitmaa, J. and W. Zhang, *Series Expansion Methods for Strongly Interacting Lattice Models* (Cambridge University Press, Cambridge, England, 2006).

[13] M. Rigol, T. Bryant, and R. R. P. Singh, Phys. Rev. Lett. **97**, 187202 (2006); Phys. Rev. E **75**, 061118 (2007).

[14] M. Rigol, T. Bryant, and R. R. P. Singh, Phys. Rev. E **75**, 061119 (2007).

[15] L. De Leo, C. Kollath, A. Georges, M. Ferrero, and O. Parcollet, Phys. Rev. Lett. **101**, 210403 (2008).

[16] T.-L. Ho and Q. Zhou, PNAS **106**, 6916 (2009).

[17] F. Heidrich-Meisner, S. R. Manmana, M. Rigol, A. Muramatsu, A. E. Feiguin, and E. Dagotto, Phys. Rev. A **80**, 041603 (2009).

[18] R. Blankenbecler, D. J. Scalapino, and R. L. Sugar, Phys. Rev. D **24**, 2278 (1981).

[19] A. Georges, G. Kotliar, W. Krauth, and M. J. Rozenberg, Rev. Mod. Phys. **68**, 13 (1996).

[20] M. H. Hettler, A. N. Tahvildar-Zadeh, M. Jarrell, T. Pruschke, and H. R. Krishnamurthy, Phys. Rev. B **58**, R7475 (1998).

[21] M. Jarrell, Th. Maier, C. Huscroft, S. Moukouri, Phys. Rev. B **64**, 195130 (2001).

[22] See the supplementary materials.

[23] A.-M. Daré, L. Raymond, G. Albinet, and A.-M. S. Tremblay, Phys. Rev. B **76**, 064402 (2007).

[24] K. Mikelsons, E. Khatami, D. Galanakis, A. Macridin, J. Moreno, M. Jarrell, Phys. Rev. B **80**, 140505 (2009).

[25] J. Bonča and P. Prelovšek, Phys. Rev. B **67**, 085103 (2003).

[26] F. Werner, O. Parcollet, A. Georges, and S. R. Hassan, Phys. Rev. Lett. **95**, 056401 (2005).

[27] S. Trotzky, Y.-A. Chen, U. Schnorrberger, P. Cheinet, and I. Bloch, Phys. Rev. Lett. **105**, 265303 (2010).

[28] D. Greif, L. Tarruell, T. Uehlinger, R. Jördens, and T. Esslinger, Phys. Rev. Lett. **106**, 145302 (2011).

[29] M. Rigol, A. Muramatsu, G. G. Batrouni, and R. T. Scalettar, Phys. Rev. Lett. **91**, 130403 (2003); Opt. Commun. **243**, 33 (2004).

[30] J.-S. Bernier, C. Kollath, A. Georges, L. De Leo, F. Gerbier, C. Salomon, M. Köhl, Phys. Rev. A **79**, 061601 (2009).

[31] T. Paiva, Y. L. Loh, M. Randeria, R. T. Scalettar, and N. Trivedi, Phys. Rev. Lett. **107**, 086401 (2011).